Published OnlineFirst May 5, 2014; DOI: 10.1158/1078-0432.CCR-14-0154

Cancer Therapy: Preclinical

Clinical Cancer Research

Disruption of Follicular Dendritic Cells–Follicular Lymphoma Cross-talk by the Pan-PI3K Inhibitor BKM120 (Buparlisib)

Alba Matas-Céspedes[1], Vanina Rodriguez[1], Susana G. Kalko[2], Anna Vidal-Crespo[1], Laia Rosich[1], Teresa Casserras[2], Patricia Balsas[1], Neus Villamor[3], Eva Giné[4], Elías Campo[3], Gaël Roué[1], Armando López-Guillermo[4], Dolors Colomer[1,3], and Patricia Pérez-Galán[1]

Abstract

Purpose: To uncover the signaling pathways underlying follicular lymphoma–follicular dendritic cells (FL–FDC) cross-talk and its validation as new targets for therapy.

Experimental Design: FL primary cells and cell lines were cocultured in the presence or absence of FDC. After 24 and 48 hours, RNA was isolated from FL cells and subjected to gene expression profiling (GEP) and data meta-analysis using DAVID and GSEA softwares. Blockade of PI3K pathway by the pan-PI3K inhibitor BKM120 (buparlisib; Novartis Pharmaceutical Corporation) and the effect of PI3K inhibition on FL–FDC cross-talk were analyzed by means of ELISA, RT-PCR, human umbilical vein endothelial cell tube formation, adhesion and migration assays, Western blot, and *in vivo* studies in mouse FL xenografts.

Results: GEP of FL–FDC cocultures yields a marked modulation of FL transcriptome by FDC. Pathway assignment by DAVID and GSEA software uncovered an overrepresentation of genes related to angiogenesis, cell adhesion, migration, and serum-response factors. We demonstrate that the addition of the pan-PI3K inhibitor BKM120 to the cocultures was able to downregulate the expression and secretion of proangiogenic factors derived from FL–FDC cocultures, reducing *in vitro* and *in vivo* angiogenesis. Moreover, BKM120 efficiently counteracts FDC-mediated cell adhesion and impedes signaling and migration induced by the chemokine CXCL12. BKM120 inhibits both constitutive PI3K/AKT pathway and FDC- or CXCL12-induced PI3K/AKT pathway, hampers FDC survival signaling, and reduces cell proliferation of FL cells *in vitro* and in mouse xenografts.

Conclusions: These data support the use of BKM120 in FL therapy to counteract microenvironment-related survival signaling in FL cells. *Clin Cancer Res; 20(13); 3458–71. ©2014 AACR.*

Introduction

Follicular lymphoma (FL), the most frequent indolent lymphoma, results from the transformation of germinal center (GC) B cells and maintains the gene expression program of this stage of differentiation (1). However, unlike normal GC cells, roughly 85% of FLs express BCL2 as a result of the characteristic t(14;18) translocation. In some cases, FL "transforms" into an aggressive diffuse large B-cell lymphoma, and this transformation is associated with a variety of oncogenic changes (2). Besides these complex intrinsic genetic abnormalities, FL cells retain, like their normal counterpart, a strong dependence on the cellular microenvironment. The importance of the microenvironment in FL is highlighted by the association of gene expression signatures derived from nonneoplastic immune cells with disease outcome. The expression of T cells and macrophage-related genes is associated with favorable survival, whereas other macrophage subtypes or follicular dendritic cells (FDC)–derived transcripts are predictive of poor outcome (3–8).

Angiogenesis plays a crucial role in oncogenesis, promoting growth and progression of both solid and hematologic tumors (9). The members of VEGF family are the most important mediators of angiogenesis and lymphangiogenesis, and this family is composed of six known members: VEGF-A (also referred as VEGF), placenta growth factor, VEGF-B, VEGF-C, VEGF-D, and VEGF-E. They interact with the corresponding receptor tyrosin kinases VEGFR-1, VEGFR-2, and VEGFR-3 and the coreceptor NRP1 (10–12). Complementary to VEGF signaling pathways, other factors participate in the angiogenic process, such as the platelet-derived growth factor (PDGF) family, indispensable

Authors' Affiliations: [1]Experimental Therapeutics in Lymphoid Malignancies Group, Department of Hemato-Oncology; [2]Bioinformatics Core Facility; [3]Hematopathology Unit, Department of Pathology; and [4]Department of Hematology, Hospital Clínic, IDIBAPS, Barcelona, Spain

Note: Supplementary data for this article are available at Clinical Cancer Research Online (http://clincancerres.aacrjournals.org/).

Corresponding Author: Patricia Pérez-Galán, IDIBAPS, Roselló 149-153, 08036 Barcelona, Spain. Phone: 349-322-75400, ext. 4525; Fax: 349-331-29407; E-mail: pperez@clinic.ub.es

doi: 10.1158/1078-0432.CCR-14-0154

Published OnlineFirst May 5, 2014; DOI: 10.1158/1078-0432.CCR-14-0154

Translational Relevance

Follicular lymphoma (FL) is the paradigm of a neoplasia depending on the microenvironment for proliferation and survival. High expression of signatures derived from follicular dendritic cells (FDC) and macrophages is associated with poor outcome. The underlying mechanisms remain ill defined and may be at the basis of disease recurrences. Here, using gene expression profiling of FL–FDC coculture systems, we have uncovered that FDCs deliver angiogenesis, adhesion, migration, and survival signaling to FL cells, and these phenomena can be counteracted by BKM120, a novel pan- PI3K inhibitor currently in clinical trials for solid tumors and hematologic malignancies. *In vitro*, BKM120 reduces proliferation, induces apoptosis, and blocks microenvironment-derived PI3K/AKT activation. *In vivo*, BKM120 reduces tumor outgrowth in subcutaneous and systemic FL mouse models and the expression of angiogenesis-related genes. These results suggest that pan-PI3K inhibitors may represent a new useful therapeutic strategy for FL interfering with microenvironment survival signaling.

for its role in vascular remodeling and maturation, and the angiopoietins (ANGPT-1, ANGPT-2, and ANGPT-4; refs. 10, 13). In FL, high mRNA levels of *VEGF-C* are more common in disseminated lymphomas, and strong nuclear expression of VEGF-C protein associates with bone marrow infiltration. Moreover, strong VEGFR-1 protein expression was found in cases with extranodal sites of involvement. Diffuse intratumoral VEGF-A staining correlated with shorter overall survival (OS) and diffuse VEGFR-2 staining was associated with a higher risk of histologic transformation (14). The role of angiogenesis in FL is further supported by two recent studies showing a correlation between increased vascularization, risk of transformation, and reduced OS (15), and an association of high $CD31^+$ microvessel density with adverse outcome of patients with FL treated with immunotherapy (16).

Patients with FL usually present with disseminated disease at diagnosis indicating the high mobility properties of these tumor cells. To enter lymphoid organs, B cells must adhere to endothelium and transmigrate across the endothelial barrier. Thus, chemokines and adhesion molecules are important in the homing of normal and malignant B cells and in lymphoma dissemination. Both firm adhesion and transmigration of the tumor cells are mediated through selectin ligands, integrins, or CD44 (17, 18). Importantly, in several models of lymphoma, including FL, the expression of several β-integrins has been associated with disease dissemination and patient prognosis (19).

However, how these observations relate to the cellular microenvironment within the lymph node is not well understood. Moreover, considering the association of FDC signatures in FL biopsies with poor outcome (5), it is of prime interest to decipher these interactions.

In the present study, we have investigated the cross-talk between FL cells and FDCs using gene expression profiling (GEP). A major contribution to angiogenesis, migration, and adhesion processes has been uncovered. Then, considering the prominent role of PI3K pathway as a common downstream transducer of these pathways (20, 21) and its known constitutive activation in FL (22–24), the effect of PI3K inhibition on these processes together with its antitumor activity in FL has been analyzed.

Materials and Methods

Cell lines and patient samples

Primary FL cells isolated from lymph nodes or peripheral blood of 11 patients (see clinical characteristics in Supplementary Table S1), diagnosed according to the World Health Organization classification criteria, were used. Written informed consent was obtained in accordance with the Ethics Committee of the Hospital Clínic, University of Barcelona and the Declaration of Helsinki. Mononuclear cells were isolated by gradient centrifugation on Ficoll (GE healthcare) and used fresh or cryopreserved in liquid nitrogen in RPMI 1640 (Life Technologies) containing 10% DMSO (Sigma-Aldrich) and 60% heat-inactivated FBS (Life Technologies), and conserved within the Hematopathology collection of our institution (IDIBAPS-Hospital Clínic Biobank). The percentage of tumor cells was evaluated by flow cytometry as $CD20^+$ $CD10^+$ showing light chain restriction lymphocytes. FL cell lines WSU-FSCCL, DOHH2, SC-1, and RL, all bearing t(14:18), were obtained from DSMZ. FL primary samples and cell lines were cultured in RPMI 1640 supplemented with 10% to 20% FBS, 2 mmol/L L-glutamine, 50 μg/mL penicillin/streptomycin and were maintained in a humidified atmosphere at 37°C containing 5% CO_2. A total of 100 μg/mL normocin (Lonza) was added to the cell line cultures to prevent Mycoplasma contamination, and were routinely tested for *Mycoplasma* infection by PCR. The identity of all cell lines was verified by using the AmpFISTR identifier Kit (Life Technologies).

FDC–FL cell coculture experiments

The follicular dendritic cell line (FDC) HK, kindly provided by Dr. Yong Sung Choi (Alton Ochsner Medical Foundation, New Orleans, LA) (25), was cultured in Iscove's modified Dulbecco's medium (Life Technologies) supplemented with 20% FBS, 2 mmol/L L-glutamine, and 50 μg/mL penicillin/streptomycin. FDC-HK cells were seeded on day 0, and FL cells ($1–2 \times 10^6$ cells/mL) were added the following day onto confluent stroma layers at 1:10 ratio (FDC:FL) and cultured for the times indicated in the presence or absence of BKM120 (buparlisib; Novartis Pharmaceutical Corporation). After the incubation times, FL primary cells were purified using CD20 magnetic beads (Miltenyi Biotech).

Gene expression profiling and data meta-analysis

Total RNA was isolated from FL cells using the TRIzol reagent (Life Technologies) followed by a cleaning step using the RNAeasy Kit (Invitrogen). RNA integrity was

Published OnlineFirst May 5, 2014; DOI: 10.1158/1078-0432.CCR-14-0154

examined with the Agilent 2100 Bioanalyzer (Agilent Technologies). Only high-quality RNA was then retrotranscribed to cDNA and hybridized on HGU219 microarray. All samples were simultaneously run in a GeneTITAN platform (Affymetrix). Principal component analysis (PCA) was done with Partek Genomics Suite. For the identification of differentially expressed genes, MEV platform (v4.9) and Rank Products test (26) were used, applying a paired analysis with an FDR of $\leq$0.05. Functional annotation of enrichment analysis was done using Database for Annotation, Visualization and Integrated Discovery (DAVID) v6.7 (NIAID, NIH). GO_FAT_BP terms with an FDR of $\leq$0.05 were considered significant. Further validation of these pathways was done using gene set enrichment analysis (GSEA) v2.0 (Broad Institute) interrogating C2 and C3 gene sets from the Molecular Signature Database v2.5, and experimentally derived custom gene sets (27). A two-class analysis with 1,000 permutations of gene sets and a weighted metric was used. Bonferroni correction for multiple testing was applied, and only gene sets with an FDR of $\leq$0.05 and a normalized enrichment score (NES) of $\geq$1.5 were considered significant. The leading edge genes were displayed using Cluster (v2.11) and TreeView (v1.6) softwares (Eisen Laboratory). The microarray data have been deposited in the NCBI's Gene Expression Omnibus and are accessible through GEO series accession number GSE54158 (http://www.ncbi.nlm.nih.gov/geo/query/acc.cgi?acc=GSE54158).

ELISA cytokine quantification

VEGF-A and VEGF-C levels were assessed in duplicates using ELISA kits (RayBiotech) in supernatants harvested from FL primary cells (2×10^6 cells/mL) and FL cell lines (0.5×10^6 cells/mL) after the indicated treatments. The optical density at 450 nm was analyzed in a spectrophotometer (Synergy Bio-tek Instrument). A standard curve was obtained by creating the serial dilution of the standards provided in the kit and used to calculate sample concentrations.

Human umbilical vein endothelial cell tube formation assay

Human umbilical vein endothelial cell (HUVEC) cells were kindly provided by Dr. Maria C. Cid (Department of Systemic Autoimmune Diseases, Hospital Clínic, IDIBAPS) and were cultured as previously described (28). Supernatants from FL primary cells (2×10^6 cells/mL) and FL cell lines (0.5×10^6 cells/mL) were harvested after 48 hours of incubation with drugs and/or in coculture with FDC-HK. 24-well plates were coated with Matrigel (Becton Dickinson) and allowed to polymerize for 30 minutes at 37°C. Afterwards, the supernatants of interest were mixed (1:1) with HUVEC cells (0.4×10^6 cells) in its medium and incubated for 24 hours. Then, the number of branch points was quantified in five randomly chosen fields. Photos were taken at $\times$40 magnification in a DMIL LED Leica microscope coupled to a DFC295 camera and analyzed with Suite v 3.7 software (Leica).

Adhesion assay

EIA/RIA 96-well plates (Costar) were coated in triplicate with 100 μL of RPMI 1640 containing either BSA 1% (nonspecific adhesion), or 500 ng/mL VCAM-1(R&D Systems) or 10 μg/mL fibronectin (Millipore), and incubated overnight at 4°C. FL primary cells (2×10^6 cells/mL) were recovered after 24 hours of incubation with BKM120 and/or in coculture with FDC-HK; cells were counted and labeled with 1 μmol/L Calcein AM (Invitrogen) for 30 minutes. After washing twice the plate with PBS, 0.2×10^6 cells per well were plated and incubated for 45 minutes at 37°C. Then, the plate was washed extensively with RPMI 1640 to remove nonadhered cells. Adhered cells were lysed with 1% Triton X-100, supernatant was transferred into black plates (Thermo Scientific; Nunc), and fluorescence was measured in a spectrophotometer (Synergy Bio-Tek Instrument; excitation filter: 485 $\pm$ 20 nm; band-pass filter: 530 $\pm$ 20 nm). Data were expressed as arbitrary fluorescent units after subtraction of nonspecific adhesion from VCAM-1/fibronectin adhesion and normalized to the untreated control.

Migration assays

SDF-1α/CXCL12-induced migration was evaluated in 24-well chemotaxis chambers containing 5 μm pore size inserts (Corning, Life Science) and performed as described (29). The migration index was calculated as the ratio between cells that migrated in response to SDF-1α divided by those that passively migrated without the chemokine.

In vivo studies

CB17 SCID mice (Charles River) were inoculated subcutaneously into their right flank with RL cell line (10^7 cells per mouse) in Matrigel (1:1) (Becton Dickinson), following a protocol approved by the animal testing ethical committee of the University of Barcelona. Treatment started when tumors were palpable (day 8), and animals received a daily intraperitoneal injection of 30 mg/kg BKM120 or an equal volume of vehicle, in a 5/2 (on/off) schedule for a total of 16 days. Twenty-three days after inoculation, animals were sacrificed according to institutional guidelines, and tumor xenografts were extirpated and weighed. In addition, the shortest (s) and longest (l) diameters of the tumor were measured with external calipers, and tumor volume was calculated using the standard formula: $s^2 \times l \times 0.5$. Tumor samples were snap-frozen in optimal cutting temperature medium (Sakura Tissue Tek) or formalin fixed and included in paraffin. Tissue sections were stained for CD19 (Dako), pAKT, pRPS6 (both from Cell Signaling Technology), CD31, and VEGF (both from Santa Cruz Biotechnology) antibodies, followed by evaluation on an Olympus DP70 microscope using Cell B Basic Imaging Software (Olympus). Total protein extracts from cryopreserved tumor samples were obtained using T-PER lysis solution (Pierce), and analyzed by SDS-PAGE as described in Supplementary Methods. For the systemic FL model, 5×10^6 WSU-FSCCL cells per mice were intravenously inoculated *via* tail vein. One week later, mice were randomly assigned into cohorts

Published OnlineFirst May 5, 2014; DOI: 10.1158/1078-0432.CCR-14-0154

of 6 mice and treated orally with 30 mg/kg BKM120 or an equal volume of vehicle, in a 5/2 (on/off) schedule for a total of 5 weeks. Mice were sacrificed 3 days later, and the presence of tumor cells was macroscopically evaluated first and then by flow cytometry labeling with CD45/CD19/CD10 antibodies in an Attune acoustic cytometer (Life Technologies).

Statistical analysis

Unpaired and paired *t* tests were used to assess differences between two groups using GraphPad Prism software 4.0.

Additional methodologic details are described in Supplementary Methods.

Results

FDC activates angiogenesis, cell adhesion, migration, and serum-like responses in FL cells

To gain insights into the molecular events underlying FDC–FL cross-talk, we established coculture systems of FL primary cells and one representative FL cell line (WSU-FSCCL) with the FDC cell line HK (FDC-HK; ref. 25), and GEP of FL cells was performed after 24 and 48 hours of coculture. PCA of microarray data was able to perfectly segregate FDC-HK–cocultured FL primary cells (FL2_HK24h, FL2_HK48h, FL3_HK24h, FL3_HK48h) from those cultured in the absence of stroma (FL2_C24h, FL2_C48h, FL3_C24h, FL3_C48h), thus highlighting the marked modulation of FL transcriptome by FDC that extended up to 48 hours (Fig. 1A). As expected, the cell line WSU-FSCCL clustered separately from FL primary cultures. In this cell line, the more significant changes occurred at 24 hours (WSU_HK24h), while the modulation started to extinguish at 48 hours; thus, WSU_HK48h localizes closer to WSU_C24h and WSU_C48h than to WSU_HK24h in the PCA diagram (Fig. 1A).

To find significantly regulated genes in FL cells by FDC-HK coculture, we loaded gene expression data into Rank Products test, and we identified 1,257 genes positively regulated and 482 negatively regulated with an FDR of <0.05 (Supplementary Fig. S1). A detailed list including gene names and fold changes is included in Supplementary Table S2. Positive regulation of gene expression was much more prominent and consistent than negative regulation that did not exceed 50% and was not present in the WSU-FSCCL cell line (Supplementary Table S2). Then, we proceed with the functional annotation of both positive and negative regulated genes by DAVID. On the top list of the positively regulated genes, we found GO_terms with an FDR of <0.05 related to cell adhesion, proliferation, angiogenesis, cell migration, and extracellular matrix (ECM) reorganization, among others (Fig. 1B–D). About the negatively regulated genes, we found a reduced number of GO_terms with an FDR of <0.05, mainly related to immune response and lymphocyte activation. On the basis of the strong modulation observed, we further focused on positive regulation, and more precisely on angiogenesis, migration, and adhesion (Supplementary Table S2). Then, we further validated these findings using GSEA and interrogating C2, C3, and custom-derived databases (27). In accordance with DAVID results, custom and C2 gene sets related to angiogenesis, adhesion, and migration were enriched (FDR < 0.05 and NES $\geq$ 1.5) in FDC-HK–cocultured FL cells (Supplementary Table S3). The corresponding enrichment plots of these significant gene sets are displayed in Supplementary Fig. S2A to S2C, respectively. In addition to these enriched gene sets, GSEA analysis using C3 data base, containing motif-associated gene sets, uncovered a very prominent enrichment (FDR < 0.001 and NES $\geq$ 1.8) of serum-response factors (SRF; Supplementary Table S3). The corresponding enrichment plots are shown in Supplementary Fig. S2D.

All together, these results using independent and complementary analytical methods indicate that FDC-HK cells activate angiogenesis, adhesion, migration, and serum-like responses in FL cells.

The pan-PI3K inhibitor BKM120 counteracts angiogenesis promoted by FL–FDC cross-talk

As uncovered by GEP analysis, FDC-HK significantly modulated the expression of angiogenesis signatures in FL cells. In Fig. 2A, heatmaps displaying the leading edge genes of two representative gene sets identified by GSEA are shown. A marked upregulation (up to 2^8-fold) of genes related to angiogenesis was consistent among the samples analyzed. This modulation extended up to 48 hours in FL primary cells, whereas in the FL cell line this signaling was extinguished after 24 hours of coculture with FDC-HK (Fig. 2A). Among the regulated genes, we identified proangiogenic growth factors and its receptors (i.e., *ANGPT1*, *ENPP2*, *EPHB2*, *FGG2*, *FST*, *HGF*, *IL6*, *IL8*, *MDK*, *PTN*, *VEGFA*, *VEGFC*, *PDGFRA*, and *PDGFRB*), lymphangiogenesis markers (*VEGFC* and *CD44*), angiogenesis markers (*AMOT*, *ANGPTL2*, and *ITGAV*), and chemokines (*CXCL1*, *CXCL2*, *CXCL5*, *CXCL12*, and *CCL2*).

Then, we focused on the search of novel therapeutic strategies that may block angiogenesis together with adhesion and migration pathways. It is well documented that PI3K/AKT plays a key role in angiogenesis, both through regulation of VEGF-A and ANGPT1 expression, and as a transducer of VEGF-A–VEGFR downstream signaling (20, 21). Several PI3K isoforms are implicated in the angiogenic process (30); thus, we analyzed the potential effect of a pan-PI3K inhibitor (BKM120) as a system to block angiogenesis. We first demonstrated that effectively BKM120 inhibits both constitutive and HK-derived AKT activation. This inhibitor reduced the levels of pAKT and its downstream transducer pRPS6, both in cell lines and primary cells in a dose-dependent manner (Supplementary Fig. S3A). This effect was also observed when pAKT levels were further increased by the presence of FDC-HK cells (Supplementary Fig. S3B). Then, RNA isolated from FL cells cultured in the absence or presence of FDC-HK cells with and without BKM120 was analyzed by RT-PCR for the expression of several proangiogenic factors and receptors (ANGPT1,

Published OnlineFirst May 5, 2014; DOI: 10.1158/1078-0432.CCR-14-0154

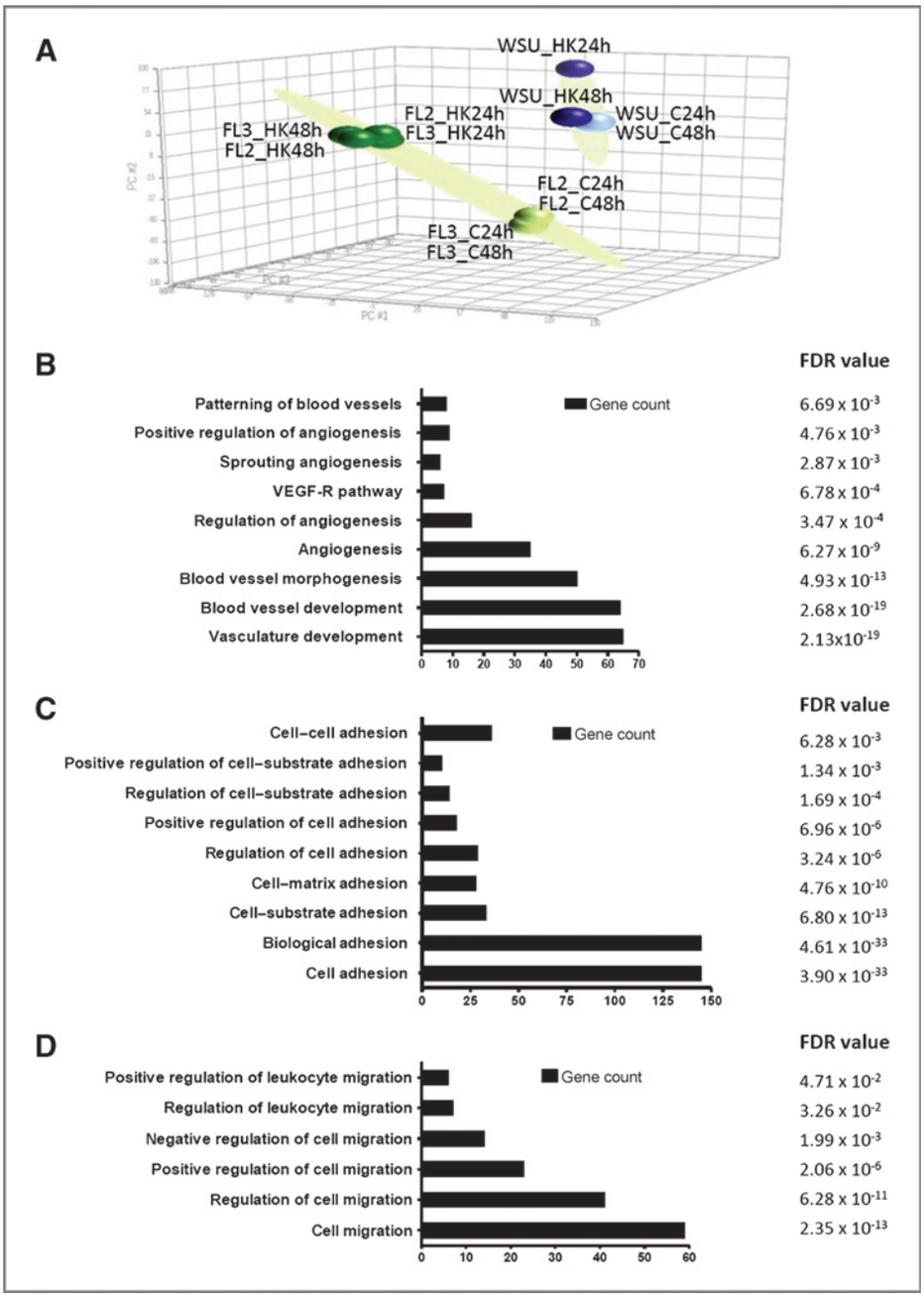

Figure 1. FDCs modify the transcriptome and deliver angiogenesis, adhesion, and migration signaling to FL cells. A, PCA of gene expression data from FL cells cocultured with the FDC cell line HK for 24 and 48 hours. DAVID functional annotation enrichment analysis of the 1,257 significant genes positively regulated with an FDR of <5%. GO terms related to angiogenesis (B), adhesion (C), and migration (D), including gene count, are shown.

VEGF-A, ENPP2, EPHB2, HGF, and NRP1) and the chemokine CXCL12. As shown in Supplementary Fig. S4, BKM120 significantly reduced the expression of those genes with the exception of ENPP2 that showed a trend.

On the basis of the central role of VEGF family on angiogenesis and lymphangiogenesis (10), we then sought to determine if the VEGF-A and VEGF-C modulation in FL cells observed by gene expression leads to an increased secretion of these factors, and the effect of PI3K inhibition on this secretion (Fig. 2B). FL primary cells alone secreted limited amounts of these factors, whereas RL cell line alone secreted higher levels of VEGF-A, in agreement with a more aggressive phenotype. FDC-HK coculture significantly increased VEGF-A ($P < 0.001$), whereas VEGF-C also increased in FL patient supernatants, but did not reach significance. Noteworthy, BKM120 was able to reduce HK-induced VEGF-A ($P < 0.01$). A similar trend was obtained for VEGF-C in FL patient supernatants that was not reproduced in the RL cell line (Fig. 2B).

Then, we further validated the effect of both FDC-HK and BKM120 on angiogenesis by a functional assay on HUVEC tube formation. As shown in Fig. 2C, supernatants from FL

Published OnlineFirst May 5, 2014; DOI: 10.1158/1078-0432.CCR-14-0154

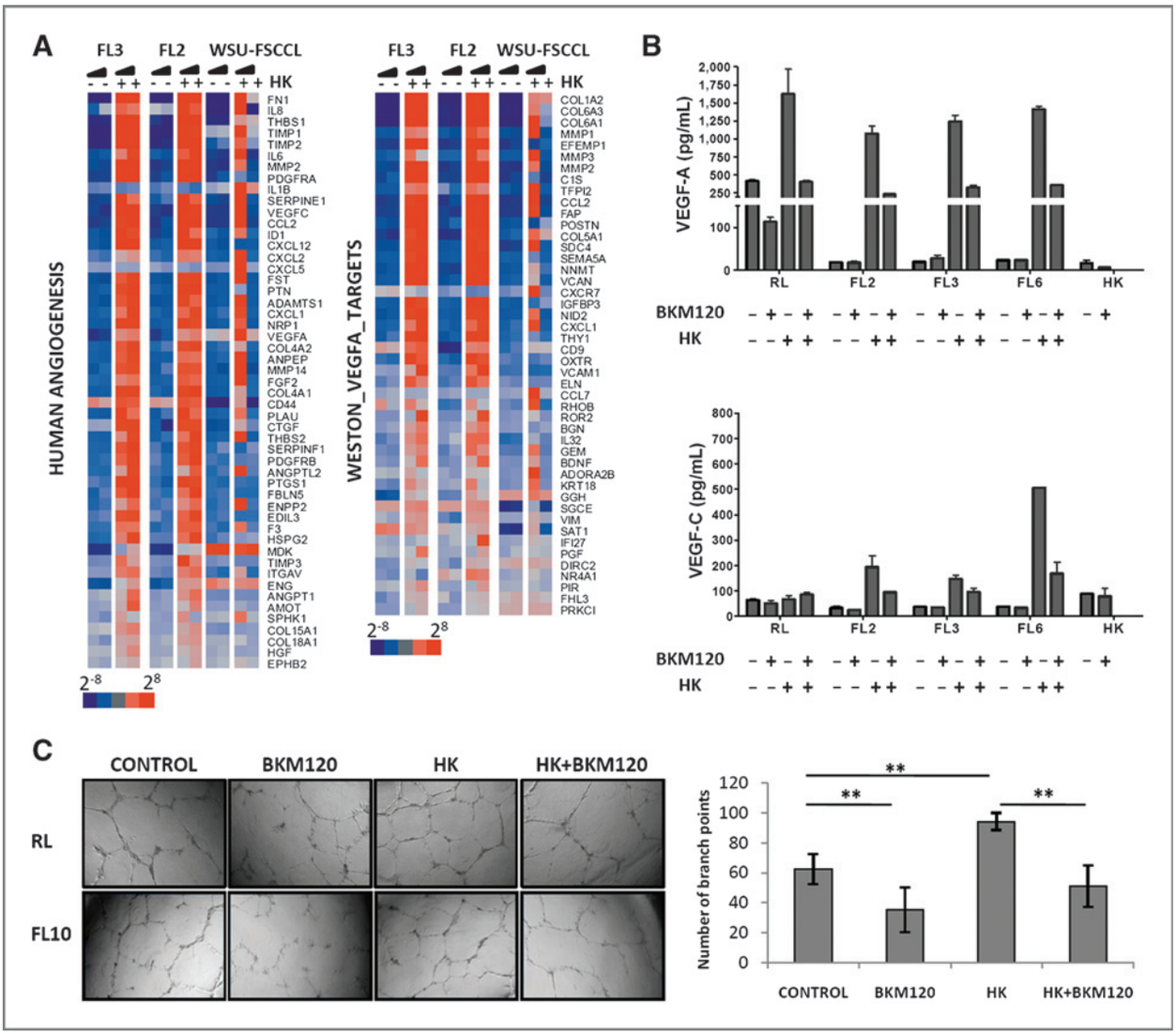

Figure 2. BKM120 interferes with FDC-induced angiogenesis. A, GSEA identifies enriched signatures related to angiogenesis. Heatmaps of the corresponding leading edge genes are shown including the relative expression of genes in FL cells cultured in the presence or absence of HK for 24 and 48 hours (this symbol represents the increasing time of incubation: 24 hours ◢ 48 hours). B, VEGF-A and VEGF-C secretion was quantified by ELISA in supernatants collected from RL cells and FL primary cells after coculture with HK cells with or without 2 μmol/L BKM120 for 24 hours (cell lines) or 48 hours (patients). HK autocrine secretion after 24 hours is also depicted. Bars correspond to the mean ± SD from duplicates. C, supernatants from RL cells and from FL primary cells ($n = 3$) after coculture with HK cells with or without 2 μmol/L BKM120 for 24 hours (cell lines) or 48 hours (patients) were added onto HUVEC cells and allowed them for tube formation during 24 hours. Microscope images from two representative cases are shown (magnification, ×40). The number of branch points was quantified as the mean of five randomly chosen fields from each well. Bars, mean ± SD of 4 FL cases. **, $P < 0.01$.

cells cocultured with FDC-HK increased the density of HUVEC tubes compared with those from control cultures, and BKM120 was able to disrupt the generation of these networks. The summary of 3 patients and one cell line is graphed, demonstrating that both FDC-HK and BKM120 effects on HUVEC tube formation were statistically significant. Taken together, these results support a role for the PI3K/AKT pathway on the angiogenesis favor by FL–FDC cross-talk and BKM120 as a potential therapeutic treatment to counteract this process.

BKM120 interferes with FDC-mediated cell adhesion to ECM elements

As uncovered by GEP analysis, FDC-HK significantly modulated the expression of adhesion-related signatures in FL cells. Heatmaps displaying the leading edges of the significantly enriched gene sets identified by GSEA are shown in Fig. 3A. Different families of molecules implicated in cell–matrix adhesion seemed to be upregulated in FL cells by FDC-HK coculture, among them: α- and β-integrins (*ITGA1*, *ITGA2*, *ITGA3 ITGA5*, *ITGA8*, *ITGB1*, *ITGB5*, and

Published OnlineFirst May 5, 2014; DOI: 10.1158/1078-0432.CCR-14-0154

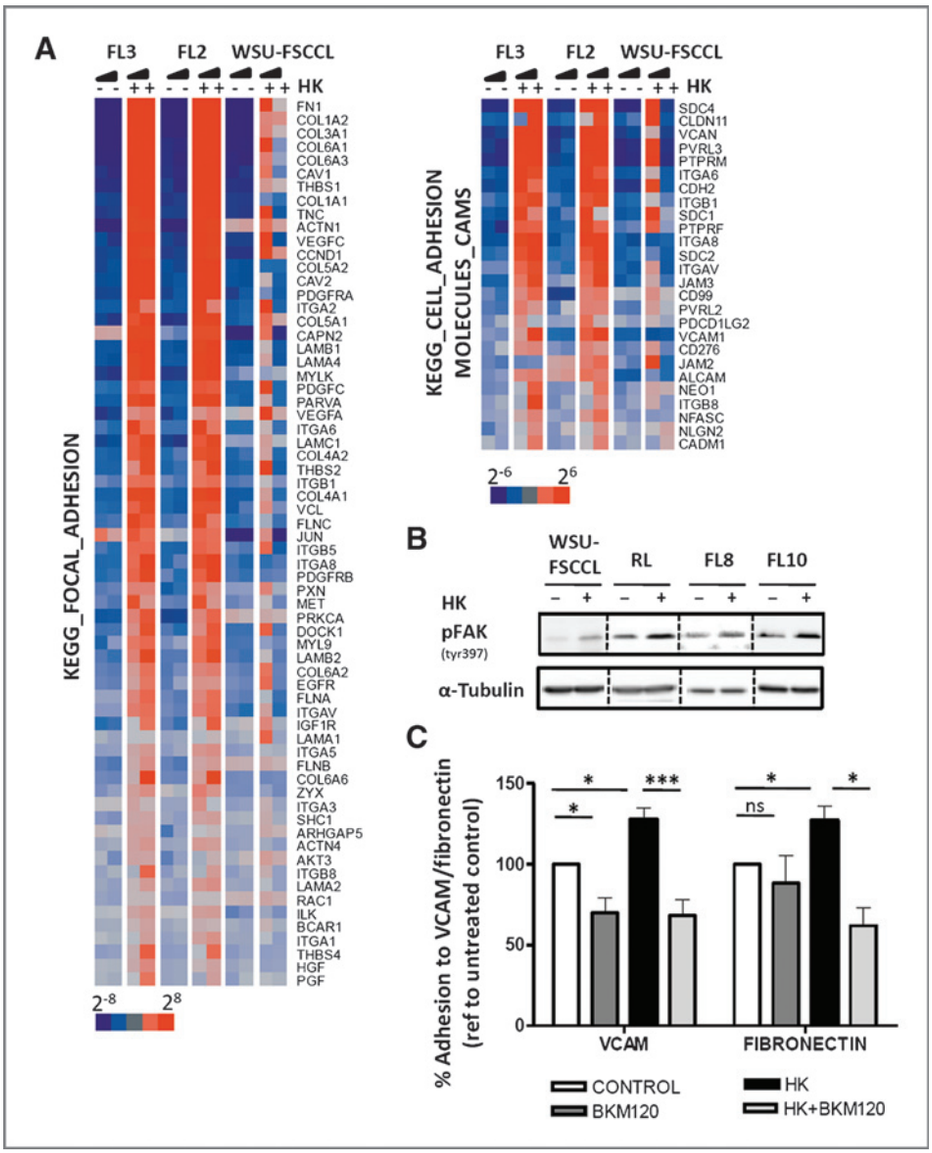

Figure 3. BKM120 reduces FDC-induced cell adhesion. A, GSEA identifies enriched signatures related to cell adhesion. Heatmaps of the corresponding leading edge are shown including the relative expression of genes in FL cells cultured in the presence or absence of HK for 24 and 48 hours (this symbol represents the increasing time of incubation: 24 hours ◢ 48 hours). B, Western blot analysis of FAK activation after coculture of FL cells for 6 hours with HK cells. C, FL primary cells ($n = 5$) were recovered after coculture with HK cells with or without 2 μmol/L BKM120 for 24 hours, and then were subjected to adhesion assays on plates precoated with BSA 1% (nonspecific adhesion), VCAM1, or fibronectin. Bars (mean ± SEM) represent the specific adhesion normalized to the corresponding untreated control without HK. *, $P < 0.05$; ***, $P < 0.001$.

ITGB8), syndecans (*SDC1*, *SDC2*, and *SDC4*), junctional adhesion molecules (*JAM2* and *JAM3*), or *CD44* (included in angiogenesis heatmaps, Fig. 2A). In the search for possible targets to interfere with this phenomenon, focal adhesion kinase (FAK) seems a critical mediator of the integrin signaling cascade, which modulates adhesion, spreading, and migration (31). As shown in Fig. 3B, FDC induced the auto-phosphorylation of FAK at residue tyrosine 397 on FL cells, a mark of activation and a docking site for Src and PI3K kinases to transmit intracellular signaling (32, 33).

On the basis of this premise, we sought to determine the impact of PI3K inhibition on intrinsic adhesion and FDC-HK–induced FL cells to ECM proteins, such as VCAM and fibronectin. Cells were cocultured for 24 hours with FDC-HK cell line in the presence or absence of BKM120 and then challenged to adhesion assay. As illustrated in Fig. 3C, FDC-HK coculture significantly increased FL cells adhesion to both VCAM and fibronectin. Moreover, PI3K inhibition by BKM120 significantly diminished both intrinsic adhesion (just in the case of VCAM) and FDC-induced adhesion to both VCAM and fibronectin. These results demonstrate that FDC increases FL cell adhesion to ECM, and that BKM120 interferes with this phenomenon.

BKM120 hampers CXCL12/CXCR4-mediated migration and signaling

FDC-HK cells significantly modulated the expression of gene sets related to cell migration (Fig. 1D and Supplementary Fig. S2C). In Fig. 4A, the leading edge of the signatures identified by GSEA is shown. Among the genes modulated, CXCL12 (mean fold change 24 h (FDC-HK vs. C) = 31.9) stands out as a prominent factor in chemotactic responses. Both lymphoma cells and stromal cells, including FDCs, secrete CXCL12 (34, 35). Moreover, drug-resistant cancer

Published OnlineFirst May 5, 2014; DOI: 10.1158/1078-0432.CCR-14-0154

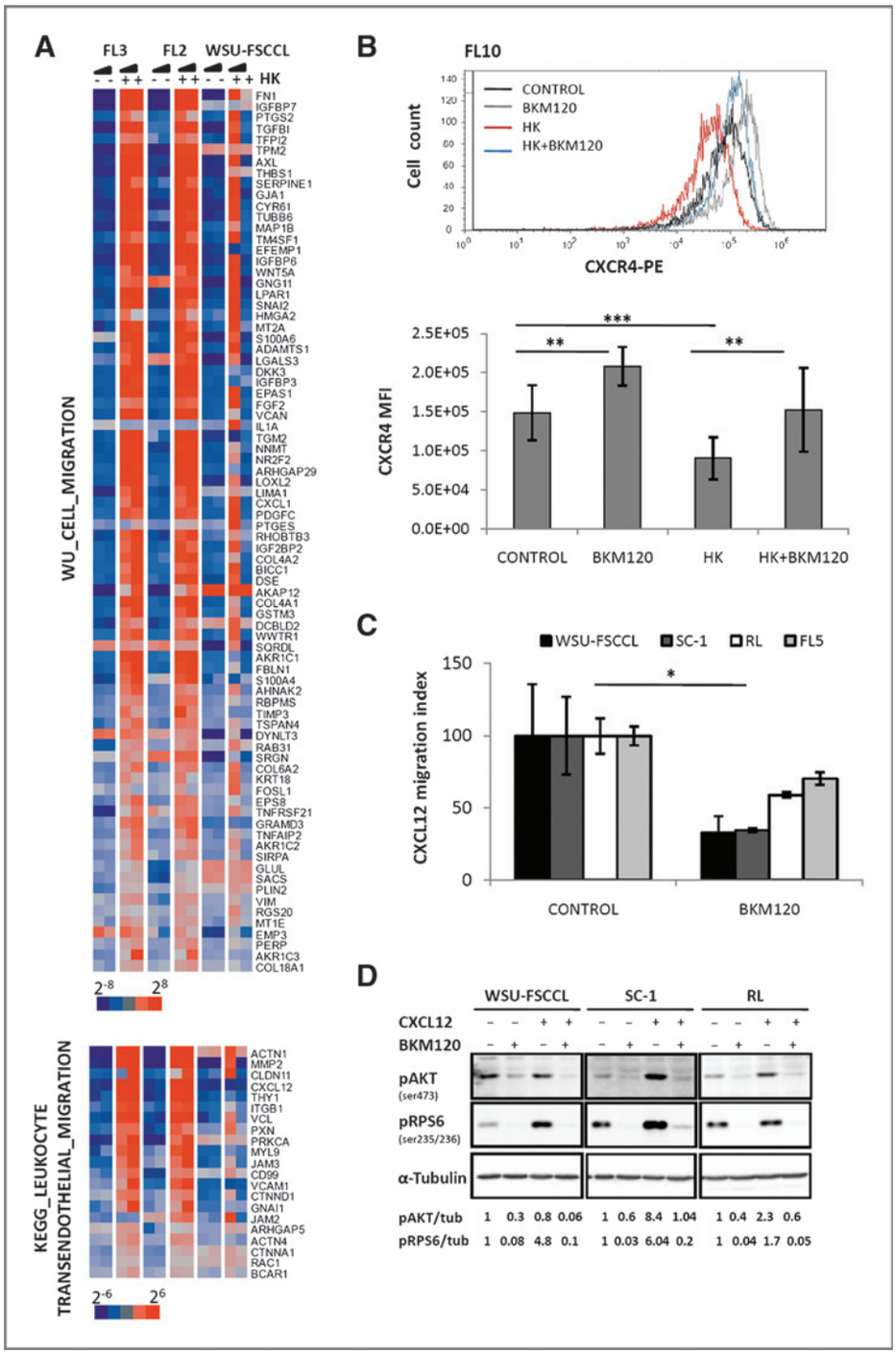

Figure 4. BKM120 interferes with CXCL12-induced migration and signaling. A, GSEA identifies enriched signatures related to cell migration. Heatmaps of the corresponding leading edges are shown including the relative expression of genes in FL cells cultured in the presence or absence of HK for 24 and 48 hours (this symbol represents the increasing time of incubation: 24 hours ◢ 48 hours). B, flow cytometry analysis of CXCR4 expression in FL primary cells ($n = 4$) and WSU-FSCCL cell line after coculture with HK cells with or without 2 μmol/L BKM120 for 24 hours. A representative flow cytometry histogram is shown. The MFI of all the cases analyzed was averaged ($n = 5$) and depicted in a bar graph (mean ± SD). C, FL cells were preincubated with 2 μmol/L BKM120 for 1 hour and then were assayed for migration in a CXCL12 gradient for 4 hours. Migration index is represented as the ratio between cells that migrated in response to CXCL12 divided by those that passively migrated without the chemokine. Bars correspond to the mean ± SD from triplicates. D, Western blot analysis of PI3K/AKT pathway activation after stimulation of FL cell lines for 30 minutes with CXCL12 and pretreated or not with 2 μmol/L BKM120 for 1 hour. Densitometric quantification of pAKT and pRPS6 normalized to the loading control (α-tubulin) and referred to untreated control is shown. *, $P < 0.05$; **, $P < 0.01$; and ***, $P < 0.001$.

stem FL cells interact with FDCs in a CXCL12/CXCR4-dependent manner to resist chemotherapy (34). In addition, PI3K inhibitors targeting p110α or p110γ isoforms interfere with CXCL12-induced migration of CLL cells (36).

We then analyzed the potential inhibitory effect of the pan-PI3K inhibitor BKM120 in CXCR4/CXCL12 axis. On the basis of GEP results, FL–FDC cross-talk may result in increased CXCL12 secretion by FL cells, and presumably FDC. As a read-out of CXCL12 levels in the culture media, we used the downregulation of the surface expression of CXCR4 in FL cells that occurs upon CXCL12 ligation (37). A representative histogram for FL10 shows that CXCR4 is downregulated by FDC-HK coculture, indicating an increase in CXCL12 levels that was reverted by BKM120 (Fig. 4B). Of note, BKM120 increased CXCR4 levels in FL cells culture in the absence of stroma, indicating that

Published OnlineFirst May 5, 2014; DOI: 10.1158/1078-0432.CCR-14-0154

the inhibitor also decreases FL CXCL12-autocrine secretion. A summary of CXCR4 mean fluorescence intensity (MFI) of several FL cases is shown. Then we analyzed the effect of BKM120 in CXCL12-induced migration and signaling. Figure 4C and D demonstrates that BKM120 significantly reduced CXCL12-induced migration and activation of PI3K/AKT pathway by the reduction in pAKT and pRPS6 levels. These results indicate that BKM120 interferes with CXCL12 secretion, migration, and signaling.

BKM120 inhibits FDC-induced survival and serum-like responses

It has been described that FDC cells induce cell survival and proliferation of FL cells (38). In line with these observations, GSEA analysis of FL–FDC GEP data, besides angiogenesis, adhesion, and migration, also revealed an over representation of gene sets related to serum responses and activation of serum response transcription factors (Fig. 5A and Supplementary Table S3), especially in patient samples.

Then, we sought to determine if FDC was able to induce serum-like responses *in vitro* and increase FL cell viability. To this aim, FL cell lines were cocultured with FDC-HK cells in serum deprivation conditions, and the number of viable FL cells was quantified. As displayed in Fig. 5B, FDC-HK coculture partially reestablished the number of viable FL cells in serum deprivation conditions ($P < 0.01$), and BKM120 was able to inhibit this serum-like effect ($P < 0.05$). Moreover, in conventional serum conditions, BKM120 impaired the increase in viability delivered by FDC-HK on FL primary cells and cell lines, and induced apoptosis in these conditions (Fig. 5C). BKM120 also reduced proliferation in FL cell lines (Supplementary Fig. S5). In summary, BKM120 counteracts survival and serum-like responses derived from FDC.

BKM120 inhibits tumor outgrowth *in vivo* and diminishes the expression of angiogenesis markers

To further analyze the potential therapeutic effect of BKM120 in FL, we then proceed for *in vivo* validation of the antiangiogenic and antitumoral activities observed *in vitro*. To this aim, we developed both heterotopic (subcutaneous, RL cell line) and systemic (intravenous, WSU-FSCCL) FL mouse models. As displayed in the tumor weight graph in Fig. 6A, BKM120 inhibited RL cell line growth *in vivo* (31% on average), in a similar extent to that observed *in vitro* (Supplementary Fig. S5). Protein lysates from the tumors confirmed that PI3K/AKT pathway was efficiently blocked *in vivo*. Moreover, VEGF-A protein expression was also downregulated (Fig. 6B). We further validated these findings by IHC in tissue sections from these tumors. In agreement with Western blot results, BKM120-treated tumors showed reduced expression of pAKT, pRPS6, and VEGF-A (Fig. 6C). In addition, the staining for CD31 protein expressed in blood vessels was also diminished in treated tumors. To further validate the antiangiogenic properties of BKM120, RNA extracted from tumors was analyzed by RT-PCR using a Human Angiogenesis Array. BKM120 reduced the expression of a significant number of proangiogenic genes, including proangiogenic factors as *VEGF-A*, *VEGF-B*, *ANGPT4*, *PDGFB*, *FBLN5*, and its receptors as *NRP2*, *PDGFRA*, and *PDGFRB* (Fig. 6D). Also the blood vessel marker CD31 (*PECAM1*) was downregulated, confirming results obtained by IHC. In contrast, the angiogenesis inhibitor *LECT1* was upregulated. Genes implicated in cell proliferation (*TGFA*, *TGFB1*, and *FGF1*) and adhesion/migration (*ITGAV*, *ITGB3*, *CEACAM1*, *TGFA*, and *TGFB1*) also seemed downregulated in treated mice. Interestingly, genes related to macrophage secretion and activation (*IFNG*, *CXCL10*, and *TNF*) were downmodulated by BKM120 treatment.

About the systemic FL mouse model, as described previously (39), WSU-FSCCL–bearing mice displayed splenomegaly, and the spleen was the organ with the highest tumor cell infiltration. Liver and bone marrow were also infiltrated but to a much lesser extent (data not shown). BKM120 significantly reduced splenomegaly in treated mice (Fig. 6E). In a set of mice, whole spleen was homogenized, and the number of FL cells ($CD45^+$, $CD19^+$, $CD10^+$) was counted by flow cytometry. As displayed in Fig. 6F, BKM120 reduced the number of resident FL cells in the spleen (on average 75%), more efficiently than in the subcutaneous model of RL cell line, in agreement with *in vitro* results for WSU-FSCCL (Supplementary Fig. S5). Tissue sections from the spleens of the remaining mice were analyzed by IHC for CD19 and pRPS6 proteins. Both markers decreased in BKM120-treated tumors, further confirming the *in vivo* inhibition of PI3K/AKT pathway and the antilymphoma effect of BKM120 (Fig. 6G). These *in vivo* results highlight the potential antitumor and antiangiogenic activity of BKM120 in FL.

Discussion

FDCs are localized to the follicles of all secondary lymphoid tissues and are critically involved in germinal center development, immunoglobulin class switching, memory B-cell generation, affinity maturation, and induction of recall responses (40). In FL, the tumor cells reside and proliferate in follicular structures in close association with helper T cells and FDCs, and lymphoma cells seem to require these cellular interactions in the GC-like environment for their proliferation and survival (41), correlating the expression of FDCs signatures with poor outcome (5). In this study, we have sought to determine the signaling pathways underlying the cross-talk between FL cells and FDCs.

To overcome the practical difficulty in isolating pure FDC to mimic this GC microenvironment, we chose to use the FDC cell line HK isolated from human tonsils (38) that has been shown to have functional features of FDC in delaying apoptosis and stimulating growth and differentiation of GC B cells (42).

We chose GEP as a discovery tool using two different and complementary analytical approaches: Rank products followed by DAVID annotation and GSEA software. Both approaches yield concordant results and identified for the first time angiogenesis, migration, adhesion, and serum-like responses as the main pathways upregulated in FL cells

Published OnlineFirst May 5, 2014; DOI: 10.1158/1078-0432.CCR-14-0154

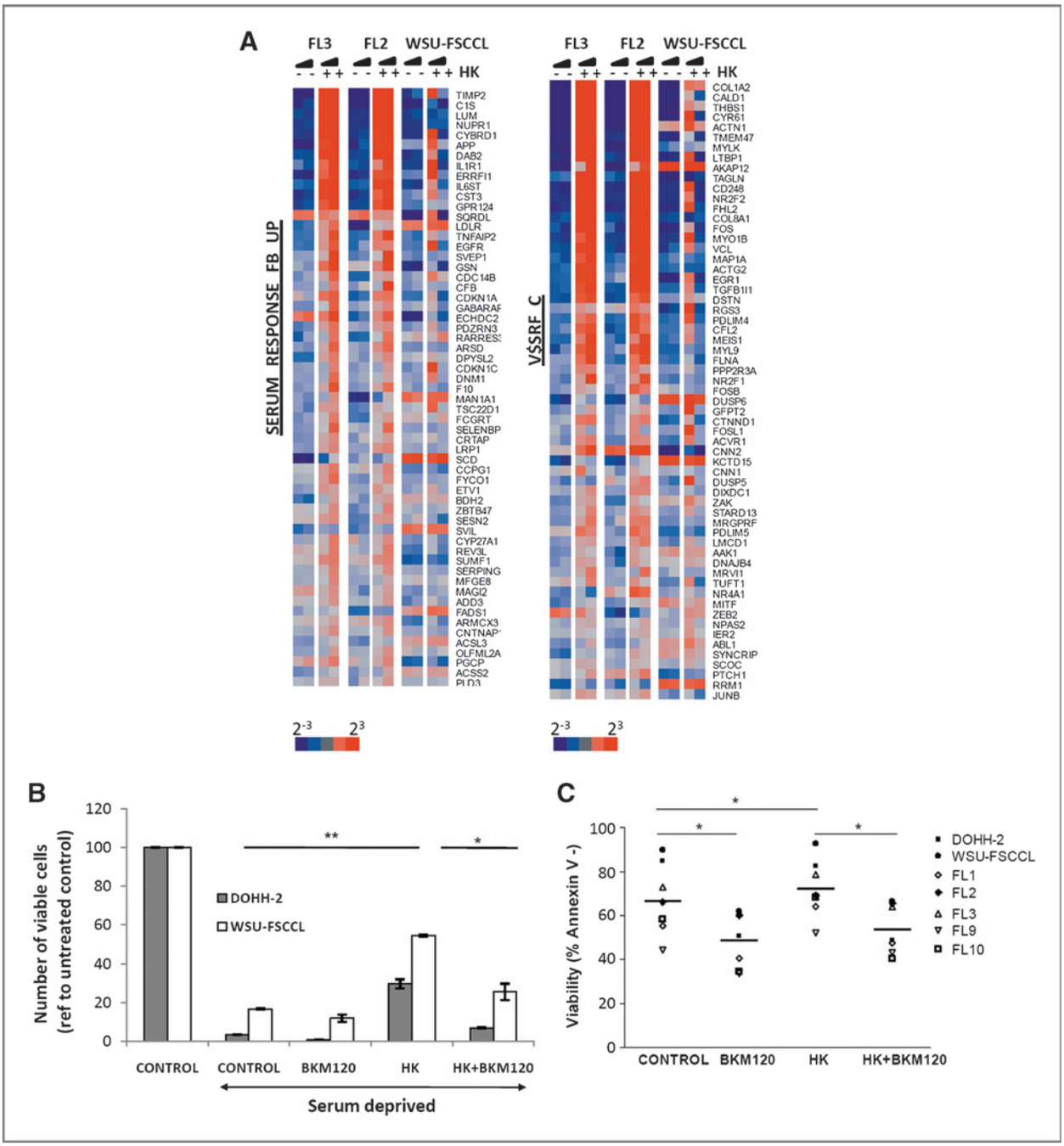

Figure 5. FDC induces serum-like responses that are mitigated by BKM120. A, GSEA identifies enriched signatures related to SRF. Heatmaps of the corresponding leading edges are shown including the relative expression of genes in FL cells cultured in the presence or absence of HK for 24 and 48 hours (this symbol represents the increasing time of incubation: 24 hours ◢ 48 hours). B, WSU-FSCCL and DOHH-2 cells were cocultured with HK cells in serum deprivation conditions (0.5% FBS) in the presence or absence of 2 μmol/L BKM120 for 72 hours. The number of viable FL cells was quantified by Annexin-V/PI and CD20 labeling. Viability is graphed and referred to the corresponding untreated control in normal culture conditions (10% FBS); bars correspond to the mean ± SD from duplicates. The line-bar between bars indicates the statistical significance considering both cell lines together.*, $P < 0.05$ and **, $P < 0.01$. C, FL primary cells ($n = 5$) and cell lines ($n = 2$) were cocultured with HK in the presence or absence of 2 μmol/L BKM120 for 48 hours, and viability was assessed by Annexin V/PI and CD20. The line-bar between dot plots shows the mean of all FL cases ($n = 7$).

upon FDC-HK coculture. These pathways may be at the basis of drug resistance and disease recurrences, and open a window of opportunity for new therapeutic avenues.

Then, we have demonstrated that PI3K pathway is a common signaling mediator of the identified pathways and may constitute a good target for therapy in this setting.

Published OnlineFirst May 5, 2014; DOI: 10.1158/1078-0432.CCR-14-0154

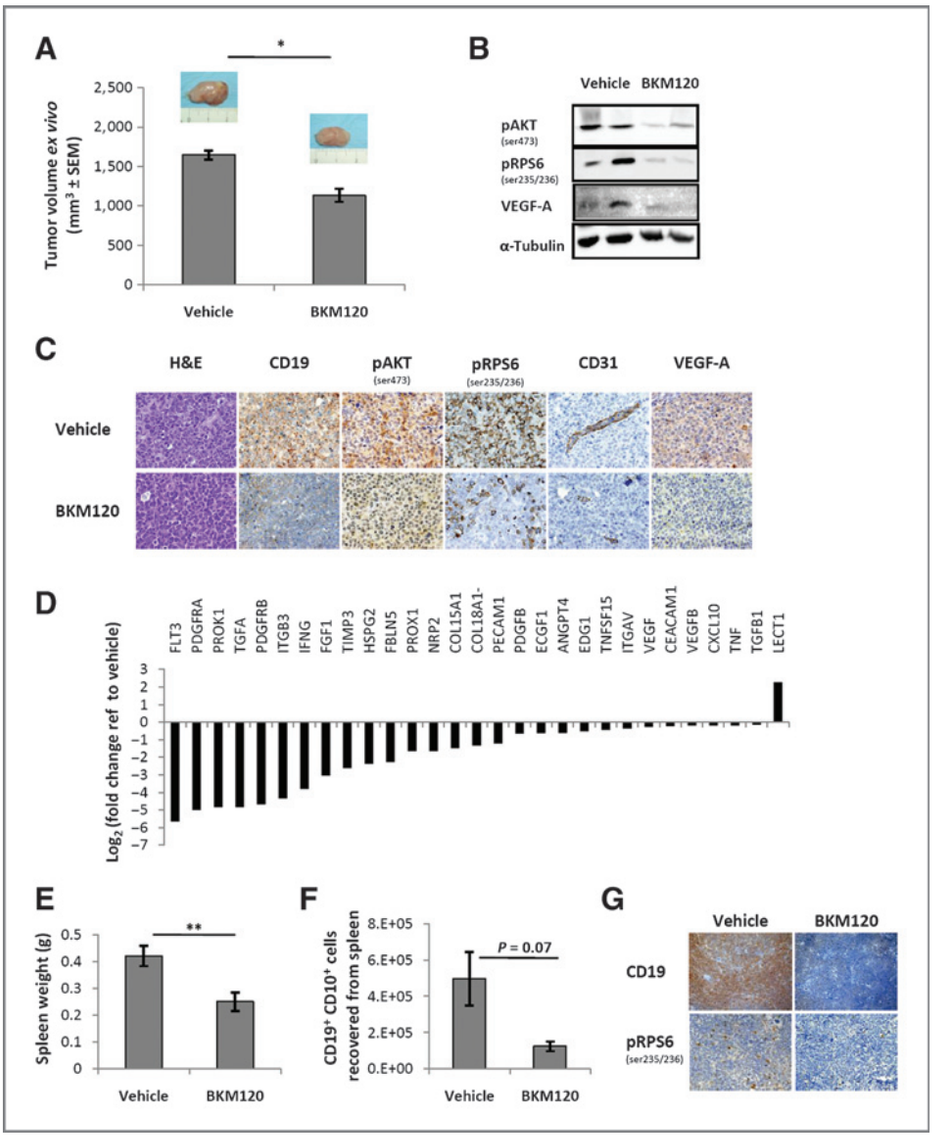

Figure 6. BKM120 reduces tumor outgrowth *in vivo* and diminishes the expression of angiogenesis factors. For the subcutaneous model, RL cells were subcutaneously inoculated into the right flank of SCID mice ($n = 2$ per group). Tumor-bearing mice received a daily intraperitoneal injection of 30 mg/kg BKM120 or an equal volume of vehicle, in a 5/2 (on/off) schedule for a total of 16 days. A, tumor size was evaluated *ex vivo* at sacrifice; bars correspond to the mean ± SEM. B, pAKT, pRPS6, and VEGF-A levels were evaluated by Western blot analysis in protein lysates obtained from the tumors of both groups. C, immunohistochemical staining of consecutive sections from tumor mass of representative specimens (magnification, ×400). Specific anti-human antibodies were used to stain CD19, pAKT, pRPS6, CD31, and VEGF-A; representative tumor pictures are shown. D, RT-PCR quantification of genes involved in angiogenesis in a representative tumor of each group, after consecutive sections from tumor mass. Bars represent the fold change referred to vehicle in $\log_2$. For the systemic model, WSU-FSCCL cells were intravenously inoculated *via* tail vein in SCID mice and treated orally with 30 mg/kg BKM120 or an equal volume of vehicle, in a 5/2 (on/off) schedule for a total of 5 weeks. Mice were sacrificed 3 days later. E, spleen size was evaluated *ex vivo* at sacrifice; bars correspond to the mean ± SEM ($n = 5$–6 per group). F, cells were recovered from the spleen, labeled with CD45/CD19/CD10, and counted in a flow cytometer. Total number of cells recovered is plotted; bars correspond to the mean ± SEM ($n = 2$–3 per group). G, immunohistochemical staining of consecutive sections from the spleen of representative specimens (magnification, ×200). Specific anti-human antibodies were used to stain CD19 and pRPS6. **, $P < 0.01$.

Two independent studies using reverse phase protein microarrays in microdissected lymphoid follicles from both FL and follicular hyperplasia identified pAKT among the strongest discriminators (23, 24), supporting AKT constitutive activation in FL and PI3K/AKT as a potential therapeutic target. As no PI3K mutations or gene amplifications have been accounted so far in FL, it is presumable that this activation derives from FL tumor cell–microenvironment interactions. Previous studies have also demonstrated the potential of PI3K/AKT/mTOR inhibitors for the treatment of GC lymphomas and their impact on angiogenesis and invasion (43, 44). In this context, we chose to work with

Published OnlineFirst May 5, 2014; DOI: 10.1158/1078-0432.CCR-14-0154

BKM120, a potent, orally available, pan-class I PI3K (45) inhibitor that has shown efficacy in *in vitro* and *in vivo* models of solid tumors and hematologic malignancies (46–48). In the clinical setting, a recently completed phase I trial in solid tumors demonstrated that BKM120 has preliminary antitumor activity (49). Likewise, BKM120 is currently being tested in a phase I trial in patients with advanced leukemias (NCT01396499) and relapsed and refractory NHL (NCT01719250), including recurrent grade 3 FL.

In this study, we have demonstrated that PI3K inhibition by BKM120 significantly reduces FDC-induced expression and secretion of proangiogenic factors in FL cell, including VEGF-A and angiopoietin 1 (ANGPT1), both required for endothelial development and to a lesser extent VEGF-C, implicated in lymphangiogenesis. Moreover, HUVEC tube formation assay using supernatants from FL–FDC-HK cocultures with or without the inhibitor formally demonstrated the antiangiogenic properties of BKM120 in FL (Fig. 2C). These results are further supported by those we obtained *in vivo*, where BKM120 also reduced VEGF-A expression and vasculature formation (Fig. 6B and C).

Interference with angiogenic process is of key importance in NHL, as several studies have pointed out its correlation with OS (14–16). The acquisition of an angiogenic phenotype, that Folkman coined in the early seventies as the "angiogenic switch" (50), results not only from interactions between vessels and cancer cells, but also involves non-neoplastic cells in the microenvironment, which may favor the development of the "angiogenic niche." In this study, for the first time, we have formally demonstrated the contribution of FDC–FL interactions to this "angiogenic niche" and that targeting PI3K pathway with BKM120 disrupts this cross-talk. It is important to highlight that compared with classical antiangiogenic agents, such as the well-characterized antibody against VEGF-A bevacizumab (Avastin), BKM120 on top of antiangiogenic properties, also offers antiproliferative activity in FL that bevacizumab lacks (data not shown). Moreover, we have also demonstrated that BKM120 hampers FDC-derived serum-like responses and survival signaling (Fig. 5B and C). In addition to angiogenesis and proliferation, this study has also uncovered that FDCs increase the motility properties of FL cells and consequently lymphoma dissemination, by two complementary mechanisms: first, by increasing the expression of adhesion molecules, which favor the previous step to migration that is ECM adhesion (17, 18), and second, by secreting chemotactic molecules such as CXCL12. In this scenario, in which FDC promotes FL dissemination, BKM120 also shows inhibitory activity. By one hand, BKM120 significantly reduces FL adhesion to ECM (VCAM and fibronectin, Fig. 3C) and reduces CXCL12 secretion and induced migration and signaling (Fig. 4B–D).

In summary, this work illustrates how FDCs contribute to FL lymphomagenesis through the modulation of a plethora of events leading to lymphoma growth and dissemination, and how inhibition of PI3K/AKT axis could interfere with this cross-talk and constitute a valuable therapeutic tool. Our results set the basis for future therapeutic approaches combining BKM120 with common treatments in FL, such as anti-CD20 monoclonal antibodies, bendamustine, or lenalidomide.

Disclosure of Potential Conflicts of Interest

No potential conflicts of interest were disclosed.

Authors' Contributions

Conception and design: A. Matas-Céspedes, P. Pérez-Galán
Development of methodology: A. Matas-Céspedes, L. Rosich, P. Pérez-Galán
Acquisition of data (provided animals, acquired and managed patients, provided facilities, etc.): A. Matas-Céspedes, V. Rodriguez, N. Villamor, E. Gine, G. Roué, A. López-Guillermo, P. Pérez-Galán
Analysis and interpretation of data (e.g., statistical analysis, biostatistics, computational analysis): A. Matas-Céspedes, S.G. Kalko, T. Casserras, A. López-Guillermo, P. Pérez-Galán
Writing, review, and/or revision of the manuscript: A. Matas-Céspedes, V. Rodriguez, A. Vidal-Crespo, L. Rosich, P. Balsas, N. Villamor, E. Gine, E. Campo, G. Roué, D. Colomer, P. Pérez-Galán
Administrative, technical, or material support (i.e., reporting or organizing data, constructing databases): A. Matas-Céspedes, V. Rodriguez, P. Pérez-Galán
Study supervision: A. Matas-Céspedes, P. Pérez-Galán

Acknowledgments

The authors thank Jocabed Roldán, Laura Jiménez, and Sandra Cabezas for their technical support, Novartis for providing BKM120, and Maria C. Cid for providing HUVEC cells and for her helpful advice on tube formation experiments. This work was carried out at the Esther Koplowitz Center, Barcelona.

Grant Support

This research was supported by the Spanish Ministry of Economy and Competitivity [RYC2009-05134 and SAF11/29326 (to P. Pérez-Galán); SAF12/31242 and IPT.2012-0673-010000 (to D. Colomer); and PI12/01847 (to G. Roué)], Redes Temáticas de Investigación Cooperativa de Cáncer from the Instituto de Salud Carlos III (ISCIII), Spanish Ministry of Economy and Competitiveness & European Regional Development Fund (ERDF) "Una manera de hacer Europa" [RD12/0036/0004 (to D. Colomer), RD12/0036/0036 (to E. Campo), and RD12/0036/0023 (to A. López-Guillermo)], and Generalitat de Catalunya (2009SGR967, to D. Colomer).

The costs of publication of this article were defrayed in part by the payment of page charges. This article must therefore be hereby marked *advertisement* in accordance with 18 U.S.C. Section 1734 solely to indicate this fact.

Received January 20, 2014; revised April 3, 2014; accepted April 27, 2014; published OnlineFirst May 5, 2014.

References

1. Alizadeh AA, Eisen MB, Davis RE, Ma C, Lossos IS, Rosenwald A, et al. Distinct types of diffuse large B-cell lymphoma identified by gene expression profiling. Nature 2000;403:503–11.
2. Lossos IS, Levy R. Higher grade transformation of follicular lymphoma: phenotypic tumor progression associated with diverse genetic lesions. Semin Cancer Biol 2003;13:191–202.
3. Carreras J, Lopez-Guillermo A, Fox BC, Colomo L, Martinez A, Roncador G, et al. High numbers of tumor-infiltrating FOXP3-positive regulatory T cells are associated with improved overall survival in follicular lymphoma. Blood 2006;108:2957–64.
4. Carreras J, Lopez-Guillermo A, Roncador G, Villamor N, Colomo L, Martinez A, et al. High numbers of tumor-infiltrating programmed cell

Published OnlineFirst May 5, 2014; DOI: 10.1158/1078-0432.CCR-14-0154

death 1-positive regulatory lymphocytes are associated with improved overall survival in follicular lymphoma. J Clin Oncol 2009;27:1470–6.
5. Dave SS, Wright G, Tan B, Rosenwald A, Gascoyne RD, Chan WC, et al. Prediction of survival in follicular lymphoma based on molecular features of tumor-infiltrating immune cells. N Engl J Med 2004;351:2159–69.
6. Glas AM, Kersten MJ, Delahaye LJ, Witteveen AT, Kibbelaar RE, Velds A, et al. Gene expression profiling in follicular lymphoma to assess clinical aggressiveness and to guide the choice of treatment. Blood 2005;105:301–7.
7. Glas AM, Knoops L, Delahaye L, Kersten MJ, Kibbelaar RE, Wessels LA, et al. Gene-expression and immunohistochemical study of specific T-cell subsets and accessory cell types in the transformation and prognosis of follicular lymphoma. J Clin Oncol 2007;25:390–8.
8. Harjunpaa A, Taskinen M, Nykter M, Karjalainen-Lindsberg ML, Nyman H, Monni O, et al. Differential gene expression in non-malignant tumour microenvironment is associated with outcome in follicular lymphoma patients treated with rituximab and CHOP. Br J Haematol 2006;135:33–42.
9. Ribatti D, Nico B, Ranieri G, Specchia G, Vacca A. The role of angiogenesis in human non-Hodgkin lymphomas. Neoplasia 2013;15:231–8.
10. Ferrara N, Gerber HP, LeCouter J. The biology of VEGF and its receptors. Nat Med 2003;9:669–76.
11. De RH, Van ME, Van CB, Vanderkerken K. Angiogenesis and the role of bone marrow endothelial cells in haematological malignancies. Histol Histopathol 2004;19:935–50.
12. Dias S, Hattori K, Zhu Z, Heissig B, Choy M, Lane W, et al. Autocrine stimulation of VEGFR-2 activates human leukemic cell growth and migration. J Clin Invest 2000;106:511–21.
13. Fagiani E, Christofori G. Angiopoietins in angiogenesis. Cancer Lett 2013;328:18–26.
14. Jorgensen JM, Sorensen FB, Bendix K, Nielsen JL, Funder A, Karkkainen MJ, et al. Expression level, tissue distribution pattern, and prognostic impact of vascular endothelial growth factors VEGF and VEGF-C and their receptors Flt-1, KDR, and Flt-4 in different subtypes of non-Hodgkin lymphomas. Leuk Lymphoma 2009;50:1647–60.
15. Farinha P, Kyle AH, Minchinton AI, Connors JM, Karsan A, Gascoyne RD. Vascularization predicts overall survival and risk of transformation in follicular lymphoma. Haematologica 2010;95:2157–60.
16. Taskinen M, Jantunen E, Kosma VM, Bono P, Karjalainen-Lindsberg ML, Leppa S. Prognostic impact of CD31-positive microvessel density in follicular lymphoma patients treated with immunochemotherapy. Eur J Cancer 2010;46:2506–12.
17. Drillenburg P, Pals ST. Cell adhesion receptors in lymphoma dissemination. Blood 2000;95:1900–10.
18. Pals ST, Drillenburg P, Radaszkiewicz T, Manten-Horst E. Adhesion molecules in the dissemination of non-Hodgkin's lymphomas. Acta Haematol 1997;97:73–80.
19. Terol MJ, Lopez-Guillermo A, Bosch F, Villamor N, Cid MC, Campo E, et al. Expression of beta-integrin adhesion molecules in non-Hodgkin's lymphoma: correlation with clinical and evolutive features. J Clin Oncol 1999;17:1869–75.
20. Cunningham SA, Waxham MN, Arrate PM, Brock TA. Interaction of the Flt-1 tyrosine kinase receptor with the p85 subunit of phosphatidylinositol 3-kinase. Mapping of a novel site involved in binding. J Biol Chem 1995;270:20254–7.
21. Gerber HP, McMurtrey A, Kowalski J, Yan M, Keyt BA, Dixit V, et al. Vascular endothelial growth factor regulates endothelial cell survival through the phosphatidylinositol 3′-kinase/Akt signal transduction pathway. Requirement for Flk-1/KDR activation. J Biol Chem 1998;273:30336–43.
22. Calvo KR, Dabir B, Kovach A, Devor C, Bandle R, Bond A, et al. IL-4 protein expression and basal activation of Erk in vivo in follicular lymphoma. Blood 2008;112:3818–26.
23. Gulmann C, Espina V, Petricoin E III, Longo DL, Santi M, Knutsen T, et al. Proteomic analysis of apoptotic pathways reveals prognostic factors in follicular lymphoma. Clin Cancer Res 2005;11:5847–55.
24. Zha H, Raffeld M, Charboneau L, Pittaluga S, Kwak LW, Petricoin E III, et al. Similarities of prosurvival signals in Bcl-2-positive and Bcl-2-negative follicular lymphomas identified by reverse phase protein microarray. Lab Invest 2004;84:235–44.
25. Kim HS, Zhang X, Choi YS. Activation and proliferation of follicular dendritic cell-like cells by activated T lymphocytes. J Immunol 1994;153:2951–61.
26. Breitling R, Armengaud P, Amtmann A, Herzyk P. Rank products: a simple, yet powerful, new method to detect differentially regulated genes in replicated microarray experiments. FEBS Lett 2004;573:83–92.
27. Shaffer AL, Wright G, Yang L, Powell J, Ngo V, Lamy L, et al. A library of gene expression signatures to illuminate normal and pathological lymphoid biology. Immunol Rev 2006;210:67–85.
28. Kleinman HK, Cid MC. Preparation of endothelial cells. Curr Protoc Cell Biol 2001;Chapter 2:Unit 2.3.
29. Chapman CM, Sun X, Roschewski M, Aue G, Farooqui M, Stennett L, et al. ON 01910.Na is selectively cytotoxic for chronic lymphocytic leukemia cells through a dual mechanism of action involving PI3K/AKT inhibition and induction of oxidative stress. Clin Cancer Res 2012;18:1979–91.
30. Jiang BH, Liu LZ. PI3K/PTEN signaling in angiogenesis and tumorigenesis. Adv Cancer Res 2009;102:19–65.
31. Zhao X, Guan JL. Focal adhesion kinase and its signaling pathways in cell migration and angiogenesis. Adv Drug Deliv Rev 2011;63:610–5.
32. Chen HC, Guan JL. Stimulation of phosphatidylinositol 3′-kinase association with foca adhesion kinase by platelet-derived growth factor. J Biol Chem 1994;269:31229–33.
33. Reiske HR, Kao SC, Cary LA, Guan JL, Lai JF, Chen HC. Requirement of phosphatidylinositol 3-kinase in focal adhesion kinase-promoted cell migration. J Biol Chem 1999;274:12361–6.
34. Lee CG, Das B, Lin TL, Grimes C, Zhang X, Lavezzi T, et al. A rare fraction of drug-resistant follicular lymphoma cancer stem cells interacts with follicular dendritic cells to maintain tumourigenic potential. Br J Haematol 2012;158:79–90.
35. Corcione A, Ottonello L, Tortolina G, Facchetti P, Airoldi I, Guglielmino R, et al. Stromal cell-derived factor-1 as a chemoattractant for follicular center lymphoma B cells. J Natl Cancer Inst 2000;92:628–35.
36. Niedermeier M, Hennessy BT, Knight ZA, Henneberg M, Hu J, Kurtova AV, et al. Isoform-selective phosphoinositide 3′-kinase inhibitors inhibit CXCR4 signaling and overcome stromal cell-mediated drug resistance in chronic lymphocytic leukemia: a novel therapeutic approach. Blood 2009;113:5549–57.
37. Haribabu B, Richardson RM, Fisher I, Sozzani S, Peiper SC, Horuk R, et al. Regulation of human chemokine receptors CXCR4. Role of phosphorylation in desensitization and internalization. J Biol Chem 1997;272:28726–31.
38. Kagami Y, Jung J, Choi YS, Osumi K, Nakamura S, Morishima Y, et al. Establishment of a follicular lymphoma cell line (FLK-1) dependent on follicular dendritic cell-like cell line HK. Leukemia 2001;15:148–56.
39. Smith MR, Joshi I, Jin F, Obasaju C. Enhanced efficacy of gemcitabine in combination with anti-CD20 monoclonal antibody against CD20+ non-Hodgkin's lymphoma cell lines in vitro and in SCID mice. BMC Cancer 2005;5:103.
40. Allen CD, Cyster JG. Follicular dendritic cell networks of primary follicles and germinal centers: phenotype and function. Semin Immunol 2008;20:14–25.
41. Carbone A, Gloghini A, Gruss HJ, Pinto A. CD40 ligand is constitutively expressed in a subset of T cell lymphomas and on the microenvironmental reactive T cells of follicular lymphomas and Hodgkin's disease. Am J Pathol 1995;147:912–22.
42. Choe J, Li L, Zhang X, Gregory CD, Choi YS. Distinct role of follicular dendritic cells and T cells in the proliferation, differentiation, and apoptosis of a centroblast cell line, L3055. J Immunol 2000;164:56–63.
43. Bhende PM, Park SI, Lim MS, Dittmer DP, Damania B. The dual PI3K/mTOR inhibitor, NVP-BEZ235, is efficacious against follicular lymphoma. Leukemia 2010;24:1781–4.
44. Fruchon S, Kheirallah S, Al ST, Ysebaert L, Laurent C, Leseux L, et al. Involvement of the Syk-mTOR pathway in follicular lymphoma cell invasion and angiogenesis. Leukemia 2012;26:795–805.

Published OnlineFirst May 5, 2014; DOI: 10.1158/1078-0432.CCR-14-0154

45. Maira SM, Pecchi S, Huang A, Burger M, Knapp M, Sterker D, et al. Identification and characterization of NVP-BKM120, an orally available pan-class I PI3-kinase inhibitor. Mol Cancer Ther 2012;11:317–28.
46. Rosich L, Saborit-Villarroya I, Lopez-Guerra M, Xargay-Torrent S, Montraveta A, Aymerich M, et al. The phosphatidylinositol-3-kinase inhibitor NVP-BKM120 overcomes resistance signals derived from microenvironment by regulating the Akt/FoxO3a/Bim axis in chronic lymphocytic leukemia cells. Haematologica 2013;98:1739–47.
47. Zang C, Eucker J, Liu H, Coordes A, Lenarz M, Possinger K, et al. Inhibition of pan-class I phosphatidyl-inositol-3-kinase by NVP-BKM120 effectively blocks proliferation and induces cell death in diffuse large B-cell lymphoma. Leuk Lymphoma 2014;55:425–34.
48. Zheng Y, Yang J, Qian J, Zhang L, Lu Y, Li H, et al. Novel phosphatidylinositol 3-kinase inhibitor NVP-BKM120 induces apoptosis in myeloma cells and shows synergistic anti-myeloma activity with dexamethasone. J Mol Med (Berl) 2012;90:695–706.
49. Bendell JC, Rodon J, Burris HA, de JM, Verweij J, Birle D, et al. Phase I, dose-escalation study of BKM120, an oral pan-Class I PI3K inhibitor, in patients with advanced solid tumors. J Clin Oncol 2012;30:282–90.
50. Folkman J. Tumor angiogenesis: therapeutic implications. N Engl J Med 1971;285:1182–6.

Published OnlineFirst May 5, 2014; DOI: 10.1158/1078-0432.CCR-14-0154

Clinical Cancer Research

Disruption of Follicular Dendritic Cells–Follicular Lymphoma Cross-talk by the Pan-PI3K Inhibitor BKM120 (Buparlisib)

Alba Matas-Céspedes, Vanina Rodriguez, Susana G. Kalko, et al.

Clin Cancer Res 2014;20:3458-3471. Published OnlineFirst May 5, 2014.